Physics Letters B 781 (2018) 376–382

Contents lists available at ScienceDirect

Physics Letters B

www.elsevier.com/locate/physletb

Dark matter contribution to $b \to s\mu^+\mu^-$ anomaly in local $U(1)_{L_\mu - L_\tau}$ model

Seungwon Baek

School of Physics, KIAS, Seoul 02455, Republic of Korea

ARTICLE INFO

Article history:
Received 11 December 2017
Received in revised form 19 March 2018
Accepted 6 April 2018
Available online 9 April 2018
Editor: J. Hisano

ABSTRACT

We propose a local $U(1)_{L_\mu - L_\tau}$ model to explain $b \to s\mu^+\mu^-$ anomaly observed at the LHCb and Belle experiments. The model also has a natural dark matter candidate N. We introduce $SU(2)_L$-doublet colored scalar $\widetilde{q}$ to mediate $b \to s$ transition at one-loop level. The $U(1)_{L_\mu - L_\tau}$ gauge symmetry is broken spontaneously by the scalar S. All the new particles are charged under $U(1)_{L_\mu - L_\tau}$. We can obtain $C_9^{\mu,\mathrm{NP}} \sim -1$ to solve the $b \to s\mu^+\mu^-$ anomaly and can explain the correct dark matter relic density of the universe, $\Omega_{\mathrm{DM}}h^2 \approx 0.12$, simultaneously, while evading constraints from electroweak precision tests, neutrino trident experiments and other quark flavor-changing loop processes such as $b \to s\gamma$ and $B_s - \overline{B}_s$ mixing. Our model can be tested by searching for Z' and new colored scalar at the LHC and $B \to K^*\nu\overline{\nu}$ process at Belle-II.

1. Introduction

Flavor changing neutral current (FCNC) processes are sensitive probe of new physics (NP) beyond the standard model (SM), of which the $b \to s\mu^+\mu^-$ has drawn much interest recently due to anomalies observed at the LHCb and Belle experiments. A form-factor independent angular observable P_5' [1] in the decay $B^0 \to K^{*0}\mu^+\mu^-$ shows 3.7σ discrepancy in the interval $4.3 < q^2 < 8.68$ GeV^2, q^2 being dimuon invariant mass squared [2]. A global analysis of the CP-averaged angular observables indicates differences from the SM predictions at the level of 3.4σ [3]. The P_5' anomaly has also been found by Belle collaborations at the level of $2.1 - 2.6\sigma$ [4,5]. For the $B_s^0 \to \phi\mu^+\mu^-$ mode, the differential branching fraction has been found to be more than 3σ below the SM predictions in the range $1 < q^2 < 6$ GeV^2 [6]. Similar tendency has been observed in $B \to K^{(*)}\mu^+\mu^-$ [7–9], $\Lambda_b^0 \to \Lambda\mu^+\mu^-$ [10].

Most interesting observables are the ratios [11]

$$R_{K^{(*)}} \equiv \frac{\mathcal{B}(B \to K^{(*)}\mu^+\mu^-)}{\mathcal{B}(B \to K^{(*)}e^+e^-)}, \tag{1.1}$$

which are predicted to be $1 + O(m_\mu^2/m_b^2)$, representing the lepton-flavor universality (LFU) in the SM. They are theoretically very clean because the hadronic uncertainties are canceled in the ratios. The measured value R_K at LHCb in the range $1 < q^2 < 6$ GeV^2 is $0.745^{+0.090}_{-0.074}(\mathrm{stat}) \pm 0.036(\mathrm{syst})$, deviating from the SM predictions by 2.6σ [12]. Recently the LHCb also measured R_{K^*} with the results [13].

$$R_{K^*} = \begin{cases} 0.66^{+0.11}_{-0.07}(\mathrm{stat}) \pm 0.03(\mathrm{syst}) & \text{for } 0.045 < q^2 < 1.1\,\mathrm{GeV}^2, \\ 0.69^{+0.11}_{-0.07}(\mathrm{stat}) \pm 0.05(\mathrm{syst}) & \text{for } 1.1 < q^2 < 6.0\,\mathrm{GeV}^2, \end{cases}$$

showing deviations at the level of $2.1 - 2.3\sigma$ and $2.4 - 2.5\sigma$ in the two q^2 regions, respectively.

It is worth noting that these possible deviations are in the same direction *i.e.* destructive with the SM, and when combined, the discrepancy with the SM predictions is at the level of $\sim 5\sigma$ [14–19]. The $b \to s\ell^+\ell^-$ decay is described by the effective weak Hamiltonian

$$\mathcal{H}_{\mathrm{eff}} = -\frac{4G_F}{\sqrt{2}} V_{ts}^* V_{tb} \sum_i (C_i^\ell O_i^\ell + C_i^{\prime\ell} O_i^{\prime\ell}) + h.c., \tag{1.2}$$

where $O_i^{(\prime)}$'s are dimension 5 and 6 $b \to s$ transition operators, for example,

$$O_7 = \frac{e}{16\pi^2} m_b (\bar{s}\sigma^{\mu\nu} P_R b) F_{\mu\nu}, \quad O_7' = \frac{e}{16\pi^2} m_b (\bar{s}\sigma^{\mu\nu} P_L b) F_{\mu\nu},$$
$$O_9^\ell = \frac{e^2}{16\pi^2} (\bar{s}\gamma_\mu P_L b)(\bar{\ell}\gamma^\mu \ell), \quad O_9^{\prime\ell} = \frac{e^2}{16\pi^2} (\bar{s}\gamma_\mu P_R b)(\bar{\ell}\gamma^\mu \ell),$$

E-mail address: swbaek@kias.re.kr.

https://doi.org/10.1016/j.physletb.2018.04.012

$$O_{10}^{\ell} = \frac{e^2}{16\pi^2}(\bar{s}\gamma_\mu P_L b)(\bar{\ell}\gamma^\mu\gamma_5\ell),$$
$$O_{10}^{\prime\ell} = \frac{e^2}{16\pi^2}(\bar{s}\gamma_\mu P_R b)(\bar{\ell}\gamma^\mu\gamma_5\ell). \quad (1.3)$$

Writing $C_i^{\ell} = C_i^{\rm SM} + C_i^{\ell,{\rm NP}}$, the SM contribution at m_b scale is $C_7^{\rm SM} \simeq -0.294$, $C_9^{\rm SM} \simeq 4.20$, $C_{10}^{\rm SM} \simeq -4.01$. The global fits to the experimental data show that the strongest pull is obtained in the scenario with NP in C_9 only [15]. The best fit value is $C_9^{\mu} = -1.21$ with pull 5.2σ.

There are already many works incorporating NP contribution to explain the violation of LFU in $b \to s\ell^+\ell^-$ decays with tree-level Z' contributions [20–39], with leptoquarks [40–48], and with loop-processes [49–54].

In this paper we propose a NP model with local $U(1)_{L_\mu - L_\tau}$ symmetry to solve the $b \to s\mu^+\mu^-$ anomaly. This model naturally breaks LFU between e and μ because the $U(1)_{L_\mu - L_\tau}$ gauge boson couples only to $\mu(\tau)$ but not to e. The model was originally proposed by He, Joshi, Lew, and Volkas [55,56]. Many variants of $U(1)_{L_\mu - L_\tau}$ model have been studied ever since: the Z' contribution to the muon $(g-2)$ discrepancy [57], $U(1)_{L_\mu - L_\tau}$-charged dark matter (DM) [58], predictions on neutrino parameters [59], very light Z' contribution to the annihilations of DM [60]. Especially the $U(1)_{L_\mu - L_\tau}$ model has also been extended to explain $b \to s\mu^+\mu^-$ anomaly, but in different context from our model [61–66]. Our model has $U(1)_{L_\mu - L_\tau}$-charged colored scalars which we call *squark* coupling to s, b-quarks, while the ref. [62] introduces vector-like quarks. The former has one-loop contribution to $b \to s\mu^+\mu^-$, whereas the latter has tree-level contribution. Our model has also a natural dark matter candidate. It corresponds to the scenario with NP in C_9 only mentioned above, which is obtained from the Z'-penguin diagrams. There is no box-diagram contribution at one-loop level. In our model C_9 includes contribution from $b \to s$ transition which comes from quark-squark-DM Yukawa interaction as well as contribution from $U(1)_{L_\mu - L_\tau}$ gauge interactions. Although the $b \to s$ transition is strongly constrained by other quark FCNC processes such as $b \to s\gamma$ and $B_s - \bar{B}_s$, we can evade them easily in our scenario.

The paper is organized as follows. In section 2, we introduce our model. The section 3 presents the results for NP contributions to $b \to s\mu^+\mu^-$, $b \to s\gamma$, and $B_s - \overline{B}_s$ mixing and shows that we can accommodate both $b \to s\mu^+\mu^-$ anomaly and the correct relic density of DM in our universe. In the section 4 we discuss DM phenomenology. We conclude in section 5.

2. The model

We introduce a local $U(1)_{L_\mu - L_\tau}$ symmetry in addition to the SM gauge group. The second (third) generation left-handed lepton doublet and right-handed singlet, $\ell_L^\mu, \mu_R, (\ell_L^\tau, \tau_R)$, are charged under $U(1)_{L_\mu - L_\tau}$ with charge $1(-1)$. It is a well-known fact that the $U(1)_{L_\mu - L_\tau}$ is anomaly-free even without extending the SM particle content. We also introduce new particles which are charged under $U(1)_{L_\mu - L_\tau}$, a Dirac fermion N, a colored $SU(2)_L$-doublet scalar $\widetilde{q} \equiv (\widetilde{u}, \widetilde{d})^T$, and a singlet-scalar S. Since the new fermion N is a Dirac particle, the theory is free from gauge anomaly. Their charge assignments are shown in Table 1.

The Lagrangian is written as

$$\mathcal{L} = \mathcal{L}_{\rm SM} - V - \frac{1}{4}Z'_{\mu\nu}Z'^{\mu\nu} + \overline{N}(i\gamma^\mu D_\mu - M_N)N + (D_\mu\widetilde{q}^\dagger)(D^\mu\widetilde{q}) - m_{\widetilde{q}}^2\widetilde{q}^\dagger\widetilde{q} + (D_\mu S^\dagger)(D^\mu S) - \sum_{i=s,b}(y_L^i\overline{q}_L^i\widetilde{q}N + h.c.) - (\frac{f}{2}\overline{N^c}NS^\dagger + h.c.), \quad (2.1)$$

Table 1
Charge assignments of $N, \widetilde{q}$ and S under the SM gauge group and $U(1)_{L_\mu - L_\tau}$. We take $Q \neq 0, \pm 1$ to avoid N being the seesaw model right-handed neutrinos.

	New fermion	New scalars	
	N	$\tilde{q}$	S
$SU(3)_C$	**1**	**3**	**1**
$SU(2)_L$	**1**	**2**	**1**
$U(1)_Y$	0	$\frac{1}{6}$	0
$U(1)_{L_\mu - L_\tau}$	Q	$-Q$	$2Q$

where $Z'_{\mu\nu} \equiv \partial_\mu Z'_\nu - \partial_\nu Z'_\mu$ is the field strength tensor for $U(1)_{L_\mu - L_\tau}$ gauge boson Z', D_μ is the covariant derivative, and i represents the generation index. The N^c is the charge conjugate state of N. The scalar potential V including the SM Higgs parts can be written as

$$V = \lambda_H\left(H^\dagger H - \frac{v^2}{2}\right)^2 + \lambda_S\left(S^\dagger S - \frac{v_S^2}{2}\right)^2 + \lambda_{HS}\left(H^\dagger H - \frac{v^2}{2}\right)\left(S^\dagger S - \frac{v_S^2}{2}\right) + \lambda_{H\widetilde{q}}\left(H^\dagger H - \frac{v^2}{2}\right)\widetilde{q}^\dagger\widetilde{q} + \lambda'_{H\widetilde{q}}\left(H^\dagger\widetilde{q}\right)\left(\widetilde{q}^\dagger H\right) + \lambda_{S\widetilde{q}}\left(S^\dagger S - \frac{v_S^2}{2}\right)\widetilde{q}^\dagger\widetilde{q} + \lambda_{\widetilde{q}}\left(\widetilde{q}^\dagger\widetilde{q}\right)^2, \quad (2.2)$$

where H is the SM Higgs doublet, $v = \sqrt{2}\langle H^0\rangle$ and $v_S = \sqrt{2}\langle S\rangle$ are vacuum expectation values (VEVs) of the scalar fields. The field $\widetilde{q}(= (\widetilde{u}, \widetilde{d})^T)$ and N mediate the $U(1)_{L_\mu - L_\tau}$ interaction to quark sector. Although the generation, $i = d$, is allowed by the gauge symmetry in general, we neglect the interaction with the first generation in this paper, because it is irrelevant in our discussion of $b \to s\mu\mu$ transition. We assume that the down-type quarks in (2.1) are already in the mass eigenstates and that the flavor mixing due to Cabibbo–Kobayashi–Maskawa (CKM) mixing appears only in the up-quark sector, *i.e.* $d_L = d'_L, u_L = V_{\rm CKM}^\dagger u'_L$ with d'_L, u'_L being the mass eigenstates. There is mass splitting between $\widetilde{u}$ and $\widetilde{d}$ due to $\lambda'_{H\widetilde{q}}$ term:

$$m_{\widetilde{u}}^2 = m_{\widetilde{q}}^2,$$
$$m_{\widetilde{d}}^2 = m_{\widetilde{q}}^2 + \frac{1}{2}\lambda'_{H\widetilde{q}}v^2. \quad (2.3)$$

The flavored-DM scenarios where DMs have interactions with quarks or leptons in a form in (2.1) have been also studied in [25, 67–69]. Since N and N^c are mixed after S gets VEV, they are not mass eigenstates. The mass matrix of N and N^c is written as

$$\begin{pmatrix} M_N & \frac{fv_S}{\sqrt{2}} \\ \frac{fv_S}{\sqrt{2}} & M_N \end{pmatrix}. \quad (2.4)$$

The mass eigenstates are mixture of N and N^c,

$$N_- = \frac{1}{\sqrt{2}}(N - N^c),$$
$$N_+ = \frac{1}{\sqrt{2}}(N + N^c), \quad (2.5)$$

whose masses are $m_\mp = M_N \mp fv_S/\sqrt{2}$. The $N_\mp$ are two Majorana particles. The N_- state has Majorana phase π so that $N_-^c = -N_-$,

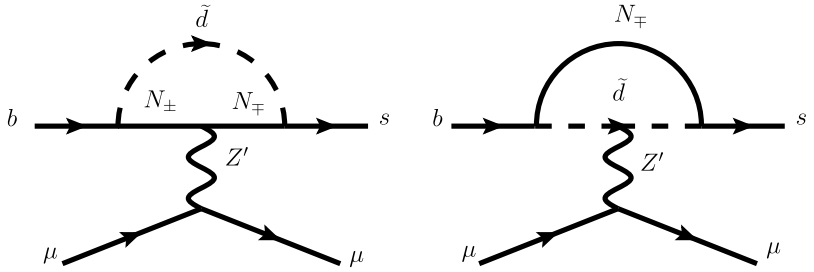

Fig. 1. Penguin diagrams generating $b \to s\mu^+\mu^-$ in our model.

but $N_+^c = N_+$. In the unitary gauge, H^0 and S can be decomposed as $H^0 = 1/\sqrt{2}(v + h)$ and $S = 1/\sqrt{2}(v_S + \phi_S)$, respectively. The scalar potential in (2.2) satisfies the tadpole conditions, $\partial V/\partial h = \partial V/\partial\phi_S = 0$, at $h = \phi_S = 0$ automatically. The mass matrix in the basis, (h, ϕ_S), is written as

$$\begin{pmatrix} 2\lambda_H v^2 & \lambda_{HS} v v_S \\ \lambda_{HS} v v_S & 2\lambda_S v_S^2 \end{pmatrix} \tag{2.6}$$

The real scalar ϕ_S mixes with the SM Higgs boson h via λ_{HS} term. The mixing angle is denoted as α_H so that

$$\begin{pmatrix} h \\ \phi_S \end{pmatrix} = \begin{pmatrix} \cos\alpha_H & \sin\alpha_H \\ -\sin\alpha_H & \cos\alpha_H \end{pmatrix} \begin{pmatrix} H_1 \\ H_2 \end{pmatrix}, \tag{2.7}$$

where $H_{1,2}$ are mass eigenstates, H_1 being the SM-like Higgs boson with mass 125 GeV.

The size of the mixing is constrained by the LHC experiments. The details can be found in [70,71]. In this work, the mixing between ϕ_S and h does not affect $b \to s\mu^+\mu^-$, but it affects the dark matter phenomenology. The direct detection experiments of dark matter strongly constrains this *Higgs portal interaction*. We take $\alpha_H \leq 0.1$ in our numerical analysis to evade the constraints from LHC experiments. We will see that it is further constrained by the DM direct detection experiments.

After $U(1)_{L_\mu - L_\tau}$ is broken by the VEV of S, v_S, there is still remnant Z_2 symmetry due to the last terms in (2.1). This discrete symmetry stabilizes the lightest neutral Z_2 odd particle, which we assume is N_-. And it becomes a good dark matter candidate. As mentioned above the DM interacts with the SM sector mediated either by the Higgs portal or Z'. The DM pair annihilates through $N_-N_- \to Z'Z'$. The coannihilation process $N_-N_+ \to Z' \to \mu^+\mu^-(\tau^+\tau^-)$ is possible in case the mass difference $\Delta m \equiv m_+ - m_- = \sqrt{2} f v_S$ is small. There is also annihilation into the SM particles through the ϕ_S and the SM Higgs mixing (Higgs portal). Notice that we take the $U(1)_{L_\mu - L_\tau}$ charge of N, $Q \neq 0, \pm 1$, so that the Yukawa interactions $\overline{\ell_L^\mu}\widetilde{H}N$ or $\overline{\ell_L^\tau}\widetilde{H}N$ ($\widetilde{H} = i\sigma^2 H^*$) are *not* allowed. Otherwise N can mix with the active neutrinos, ν_μ or ν_τ, and N cannot be the electroweak scale WIMP DM candidate.

After S gets VEV, the $U(1)_{L_\mu - L_\tau}$ gauge boson gets mass, $m_{Z'} = 2g_X|Q|v_S$, where g_X is the $U(1)_{L_\mu - L_\tau}$ gauge coupling constant. The squarks $\widetilde{u}$ and $\widetilde{d}$ have masses $m_{\widetilde{u}}^2 = m_{\widetilde{q}}^2$ and $m_{\widetilde{d}}^2 = m_{\widetilde{q}}^2 + \lambda'_{Hq} v^2/2$, respectively. Since large mass splitting leads large contribution to ρ-parameter [72] and the mass splitting does not affect the analysis, we set $\lambda'_{Hq} = 0$ for simplicity.

3. NP contribution to $b \to s$ transitions in our model

In our model the $b \to s\mu^+\mu^-$ transition operator O_9^μ is generated by Z'-exchanging penguin diagrams as shown in Fig. 1. From the diagrams we can see that only $C_9^{\mu(\tau),\mathrm{NP}}$ is generated. There is no box diagram contribution at one-loop level. The effective $b - s - Z'$ vertex reads

$$iV_{\mathrm{eff}}^\mu(q^2) \equiv -\frac{i}{(4\pi)^2} Q\, y_L^s y_L^b g_X\, \mathcal{V}_{sb}(x_-, x_+, q^2)\overline{u}(p_1)\gamma^\mu p_L u(p_2), \tag{3.1}$$

where p_1, p_2 are momenta of external s, b-quarks, $q = p_1 - p_2$, $x_\mp = m_\mp^2/m_{\widetilde{d}}^2$, and the loop-function $\mathcal{V}_{sb}(x_-, x_+, q^2)$ reduces to the analytic function $\mathcal{V}_{sb}(x_-, x_+)$ given in the appendix A in the $q^2 \to 0$ limit. Note that each of the effective vertices in Fig. 1 diverges but their sum yields a finite value. Then the amplitude for the penguin diagram contributions to $b \to s\mu^+\mu^-$ in Fig. 1 can be obtained to be

$$\begin{aligned} iA_{\mathrm{full}} &= iV_{\mathrm{eff}}^\mu(q^2)\frac{-i(g_{\mu\nu} - q_\mu q_\nu/m_{Z'}^2)}{q^2 - m_{Z'}^2}(-ig_X)\overline{v}(p_3)\gamma^\nu u(p_4) \\ &\simeq iV_{\mathrm{eff}}^\mu(0)\frac{ig_{\mu\nu}}{m_{Z'}^2}(-ig_X)\overline{v}(p_3)\gamma^\nu u(p_4), \end{aligned} \tag{3.2}$$

where we neglected small $q \sim O(m_b - m_s)$ in the second line. Comparing the full amplitude in (3.2) with the amplitude obtained from the effective Hamiltonian in (1.3), we get

$$C_9^{\mu,\mathrm{NP}} = -Q\frac{\sqrt{2}}{4G_F m_{Z'}^2}\frac{\alpha_X}{\alpha_{\mathrm{em}}}\frac{y_L^s y_L^b}{V_{ts}^* V_{tb}}\mathcal{V}_{sb}(x_-, x_+), \tag{3.3}$$

where $\alpha_X = g_X^2/(4\pi)$. In the limit $m_- = m_+$ we obtain $\mathcal{V}_{sb}(x_-, x_-) = 0$. This can be understood from the fact we took zero momentum limit to get $\mathcal{V}_{sb}(x_-, x_+)$. In the limit $m_- = m_+$, the two Majorana fermions $N_\mp$ return to the original Dirac fermion N. Note $\Delta m = \sqrt{2} f v_S = 0$ corresponds to $v_S = 0$. And the $U(1)_{L_\mu - L_\tau}$ gauge symmetry is restored, and $\mathcal{V}_{sb}(x_-, x_-) = 0$ is simply a consequence of $U(1)_{L_\mu - L_\tau}$ gauge invariance: the Ward identity, $V_{\mathrm{eff}}^\mu(q^2 = 0)q_\mu = 0$, implies $\mathcal{V}_{sb}(x_-, x_-) = 0$ because $\overline{u}(p_1)\gamma^\mu p_L u(p_2)q_\mu \neq 0$. We neglected small ratios such as $m_b^2/m_{\widetilde{d}}^2, m_s^2/m_{\widetilde{d}}^2$ to obtain the analytic formula $\mathcal{V}_{sb}(x_-, x_+)$. Therefore, to get a sizable $C_9^{\mu,\mathrm{NP}}$ we need large mass splitting Δm, which implies the DM coannihilation processes for the DM relic cannot be a dominant component in our scenario. Fig. 2 shows a contour plot for $C_9^{\mu,\mathrm{NP}}$ (blue lines) in the plane (m_-, m_+). For the plot we fixed $Q = 3/2$, $\alpha_X = 0.05$, $y_L^s y_L^b = 0.1$, $m_{Z'} = 500$ GeV, $m_{H_1} = 125$ GeV, $m_{H_2} = 1$ TeV, and $m_{\widetilde{d}} = 3$ TeV. The left (right) panel corresponds to $\alpha_H = 0.01(0.001)$. This choice of α_X and $m_{Z'}$ can be target of LHC searches for Z' [65]. In the same plot we also show $\Omega h^2 = 0.12$ lines (green and gray lines), which could explain the DM relic in the universe. The green (gray) segments are (not) allowed by the DM direct search experiments. We used the upper limit from LUX for the plot [73]. The DM phenomenology will be discussed in more detail in Section 4. We can see that $C_9^{\mu,\mathrm{NP}} \sim -1$ can be obtained with sizable mass splittings in the case $\alpha_H = 0.001$, which can explain the $b \to \mu^+\mu^-$ anomaly. Smaller α_H is preferred because it can help evade the direct search bound whereas the scalar mixing does not affect $C_9^{\mu,\mathrm{NP}}$. We also note that the value of $C_9^{\mu,\mathrm{NP}}$

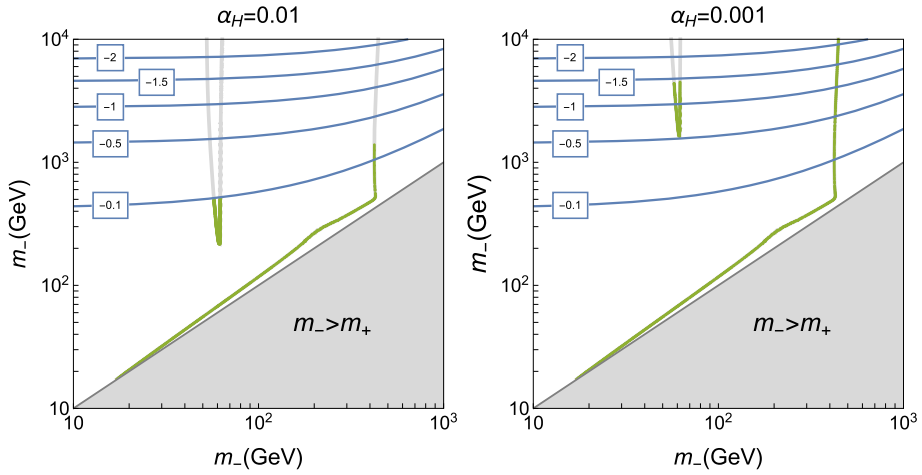

Fig. 2. Contour plot for $C_9^{\mu,\mathrm{NP}}$ at the electroweak scale (blue lines) and $\Omega h^2 = 0.12$ (green and grey lines) in the plane (m_-, m_+). We fixed $Q = 3/2$, $\alpha_X = 0.05$, $y_L^s y_L^b = 0.1$, $m_{Z'} = 500$ GeV, $m_{\widetilde{d}} = 3$ TeV, $m_{H_1} = 125$ GeV, and $m_{H_2} = 1$ TeV. We also set $\alpha_H = 0.01$ (left panel) and $\alpha_H = 0.001$ (right panel). The grey segments of the lines are excluded by the DM direct detection experiments. (For interpretation of the colors in the figure(s), the reader is referred to the web version of this article.)

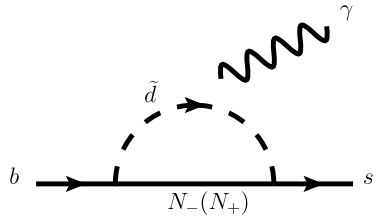

Fig. 3. Feynman diagrams for $b \to s\gamma$ in our model. The photon can be attached to electrically charged particles, $\widetilde{d}, b$ or s.

does not depend on the absolute value of $m_{\widetilde{d}}$ or $m_\mp$ but only on their ratios. We take $m_{\widetilde{d}} = 3$ TeV as a reference value.

The couplings y_L^s and y_L^b also generate other quark FCNC processes such as $b \to s\gamma$ and $B_s - \overline{B_s}$ mixing. The experimental measurement of the inclusive branching fraction of radiative B-decay, $\overline{B} \to X_s\gamma$, is [74]

$$\mathcal{B}\left[\overline{B} \to X_s\gamma, \left(E_\gamma > \frac{1}{20}m_b\right)\right]^{\mathrm{exp}} = (3.32 \pm 0.15) \times 10^{-4}, \quad (3.4)$$

which can be compared with theoretical prediction in the SM prediction [75]

$$\mathcal{B}\left[\overline{B} \to X_s\gamma, \left(E_\gamma > 1.6\,\mathrm{GeV}\right)\right]^{\mathrm{SM}} = (3.36 \pm 0.23) \times 10^{-4}. \quad (3.5)$$

The NP contribution to C_7^γ at the electroweak scale whose diagram is shown in Fig. 3 is obtained to be

$$C_7^{\gamma,\mathrm{NP}} = \frac{\sqrt{2}e_d}{16G_F m_{\widetilde{d}}^2}\frac{y_L^s y_L^b}{V_{ts}^* V_{tb}}[J_1(x_-) + J_1(x_+)], \quad (3.6)$$

where $e_d = -1/3$ is the electric charge of $\widetilde{d}$, and the loop function $J_1(x)$ is given in the Appendix A. The corresponding SM value is $C_7^{\gamma,\mathrm{SM}}(\mu_b) \simeq -0.294$ [76].

The NP contribution to $B_s - \overline{B_s}$ mixing occurs via the box diagrams shown in Fig. 4. The mass difference in the $B_s - \overline{B_s}$ system has been measured by CDF and LHCb and the average value is

$$\Delta m_s = 17.757 \pm 0.020(\mathrm{stat}) \pm 0.007(\mathrm{syst})\ \mathrm{ps}^{-1}, \quad (3.7)$$

which is in good agreement with the SM predictions [77] with predictions $17.5 \pm 1.1\ \mathrm{ps}^{-1}$ [78] or $16.73^{+0.82}_{-0.57}\ \mathrm{ps}^{-1}$ [79]. More recently the ref. [80] reports larger central value for the SM prediction but with larger errors, $\Delta m_s^{\mathrm{SM}} = 18.6^{+2.4}_{-2.3}$. The effective Hamiltonian in the SM has $(V-A)\times(V-A)$ structure since the W-boson couples only to left-handed quarks,

$$\begin{aligned}\mathcal{H}_{\mathrm{eff}}^{\Delta B=2} &= \frac{G_F m_W^2}{4\pi^2}(V_{ts}^* V_{tb})^2 S_0(x_t)\bar{s}\gamma_\mu P_L b\bar{s}\gamma^\mu P_L b \\ &\equiv C_1^{\mathrm{SM}}(\mu_W)\bar{s}\gamma_\mu P_L b\bar{s}\gamma^\mu P_L b, \end{aligned} \quad (3.8)$$

where $x_t = m_t^2/m_W^2$ and the loop function $S_0(x_t)$ can be found, *e.g.*, in [76]. The NP contribution to the $B_s - \overline{B_s}$ mixing whose Feynman diagrams are shown in Fig. 4 can also be written in the form

$$\mathcal{H}_{\mathrm{eff}}^{\Delta B=2,\mathrm{NP}} = C_1^{\mathrm{NP}}\bar{s}\gamma_\mu P_L b\bar{s}\gamma^\mu P_L b, \quad (3.9)$$

where at the electroweak scale

$$\begin{aligned} C_1^{\mathrm{NP}}(\mu_W) = \frac{(y_L^s y_L^b)^2}{128\pi^2 m_{\widetilde{d}}^2}\Big[&2k(x_-,x_-,1) + 4k(x_-,x_+,1) \\ &+ 2k(x_+,x_+,1) + x_- j(x_-,x_-,1) \\ &+ 2\sqrt{x_-x_+}\,j(x_-,x_+,1) + x_+ j(x_+,x_-,1)\Big], \end{aligned} \quad (3.10)$$

where the loop functions j and k are listed in the Appendix A. Since new particles in our model couple only to the left-handed quarks as shown in (2.1), the NP operator has the same Lorentz structure with the SM operator in (3.8).

By comparing the experimental results with the SM predictions, we can see that both $b \to s\gamma$ and $B_s - \overline{B_s}$ mixing still allows ~ 10 % contribution from NP. To see the impact of these FCNC constraints on our model, in Fig. 5 we show contour plots for $C_7^{\gamma,\mathrm{NP}}/C_7^{\gamma,\mathrm{SM}}$ for $b \to s\gamma$ and $C_1^{\mathrm{NP}}/C_1^{\mathrm{SM}}$ for $B_s - \overline{B_s}$ mixing at the electroweak scale. We take the same parameters with Fig. 2. We see the NP contribution to the $b \to s\gamma$ is typically a few$\times O(10^{-4})$ of the SM contribution and its contribution to the $B_s - \overline{B_s}$ mixing is a few % near the region where $C_9^{\mu,\mathrm{NP}} \sim -1$. Consequently we can safely evade the constraints for the parameters chosen in Fig. 2 while getting sizable $C_9^{\mu,\mathrm{NP}} \sim -1$ to resolve the $b \to s\mu\mu$ anomaly. We also checked even for the relatively large $\Delta m = \sqrt{2} f v_S$, the dark Yukawa coupling f can be still in the perturbative regime, *i.e.* $f \lesssim 4\pi$. The key observation is that the large contribution to $C_9^{\mu,\mathrm{NP}}$ comes from the relatively light Z' ($m_{Z'} \sim O(100)$ GeV) and sizable $U(1)_{L_\mu - L_\tau}$ coupling, $\alpha_X \sim 0.1$, while Z' gauge boson is not involved in $b \to s\gamma$ or $B_s - \overline{B_s}$ mixing at the one-loop level.

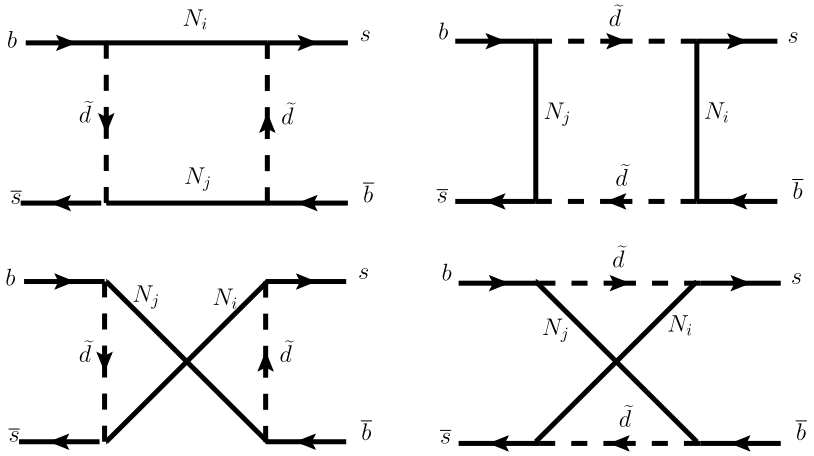

Fig. 4. Box diagrams which contribute to $B_s - \overline{B}_s$ mixing, where $i, j = \pm$.

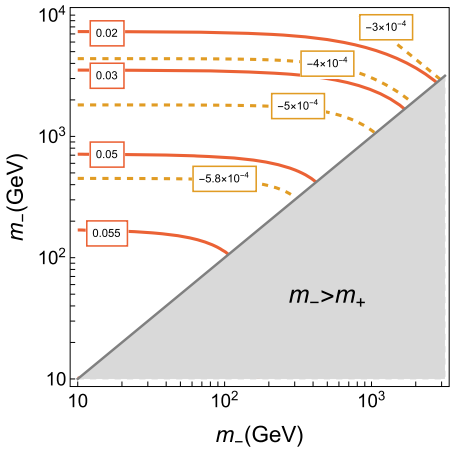

Fig. 5. Contour plots for $C_7^{\gamma,\mathrm{NP}}/C_7^{\gamma,\mathrm{SM}}$ (dashed lines) and $C_1^{\mathrm{NP}}/C_1^{\mathrm{SM}}$ (solid lines) at the electroweak scale. The fixed parameters are the same with Fig. 2.

Our model can contribute also possibly to $B \to K^{(*)}\nu\bar{\nu}$ processes. The leading diagrams are obtained by replacing μ with ν_μ and ν_τ in Fig. 1. However, since their $U(1)_{L_\mu - L_\tau}$ charges, $Q_\mu = +1$ and $Q_\tau = -1$, add to zero, the two contributions cancel with each other in the leading order of NP contributions. And the decay rates are increased only by about 2 %, making the modifications challenging to observe [61].

4. Dark matter relic density and direct detection

There are many DM annihilation diagrams for the relic density in our model: $H_1(H_2)$-mediated s-channel diagrams for $N_-N_- \to$ SM SM (Higgs portal contributions), $\tilde{d}$-mediated t-channel diagrams for $N_-N_- \to ss, sb, bb$, and $N_-N_- \to Z'Z', H_jH_k(j,k=1,2)$ which have both Higgs-mediated s-channel and $N_+(N_-)$-mediated t-channel diagrams. They are shown in Fig. 6.

Also coannihilation diagrams can make contributions when $\Delta m (= m_+ - m_-) \approx m_-/20$. To calculate the relic density and DM nucleon scattering cross section we implemented our model to the numerical package micrOMEGAs [81].

Fig. 2 shows contour lines for the total DM relic density $\Omega_{\mathrm{DM}}h^2 \approx 0.12$ (green and gray lines). We can clearly see three main contributions: i) Higgs resonance contribution dominating near $m_- \approx m_{H_1}/2 \approx 65$ GeV, ii) the coannihilation contributions are important along the line $m_+ \approx m_-$, iii) $N_-N_- \to Z'Z'$ process takes over when it is kinematically open near $m_- \gtrsim m_{Z'}$. The green (gray) segments satisfy (do not satisfy) the constraints from the DM and nucleon scattering experiments. When the coannihilation dominates, it is difficult to get sizable $C_9^{\mu,\mathrm{NP}}$, which can be seen also in Fig. 2. In the right panel the green lines with $C_9^{\mu,\mathrm{NP}} \sim -1$ intersect with the lines with $\Omega h^2 = 0.12$, while satisfying the direct detection constraints. And we can accommodate both the $R_{K^{(*)}}$ anomaly and the correct DM relic density of the universe in our model.

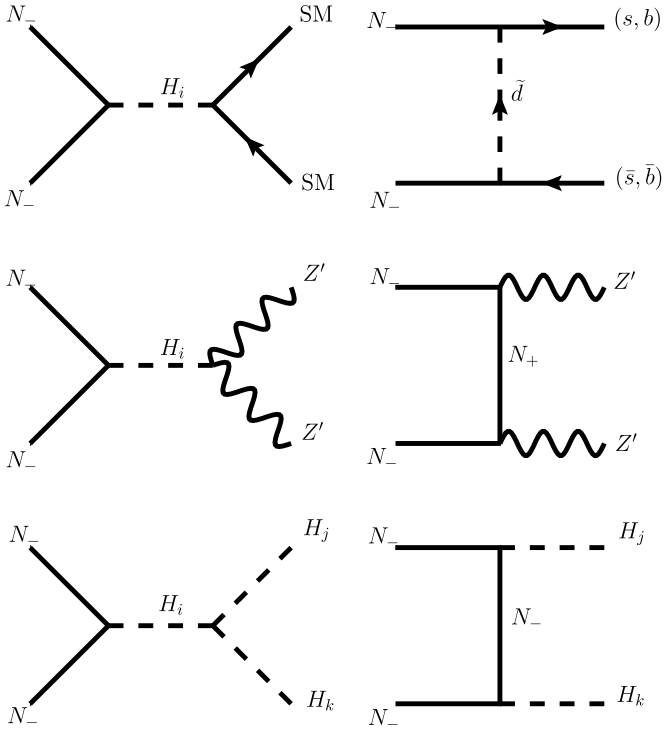

Fig. 6. DM annihilation diagrams for relic density.

The main contribution to the direct detection experiments comes from the $H_i(i=1,2)$-exchanging t-channel diagrams (Higgs portal). Since the Higgs portal contribution favors large α_H, it is clear to see that the Higgs-resonance region is more strongly constrained. By the same reason the constraint is more stringent in the left panel than the right. We note that to explain both the B-anomaly and the null search of DM with nucleon scattering the bound on α_H becomes much more stronger $\alpha_H \lesssim 0.01$ than the collider bound $\alpha_H \lesssim 0.1$.

5. Conclusions

The LHCb and Belle experiments have observed tantalizing anomalies in $b \to s\mu^+\mu^-$ processes in the observables of P_5', $R_{K^{(*)}}$ and some branching fractions. The global fits show $\sim 5\sigma$ deviation from the standard model predictions with the best fit value $C_9^{\mu,\mathrm{NP}} \sim -1$ for $C_9^{\mu,\mathrm{NP}}$ only scenario. We propose a local $U(1)_{L_\mu - L_\tau}$ model which correspond to this scenario. The model also contains a natural dark matter candidate. The new physics contribution to $b \to s$ transition occurs via the exchange of colored $SU(2)_L$-doublet scalar $\widetilde{q}$ which is also charged under $U(1)_{L_\mu - L_\tau}$. To conserve $U(1)_{L_\mu - L_\tau}$ charge in the Yukawa interaction of $\widetilde{q}$ with the SM quarks b, s, we need a Dirac fermion N which is electrically neutral but charged under $U(1)_{L_\mu - L_\tau}$ so that the Yukawa interaction takes the form $y_L^i \widetilde{q}_L^i \widetilde{q} N + h.c.$. The neutral fermion can be a dark matter candidate. The stability of dark matter candidate N is achieved by the interaction $f\overline{N^c} N S^\dagger + h.c.$ where S is $U(1)_{L_\mu - L_\tau}$-breaking scalar, which leaves exact Z_2 symmetry after S obtains vacuum expectation value. The lightest Z_2-odd neutral Majorana fermion mass eigenstate N_- becomes a stable dark matter.

The model contributes to the C_9^μ for $b \to s\mu^+\mu^-$ through the Z'-exchanging penguin diagrams. When $\alpha_X \sim 0.05$, $m_{Z'} \sim 500$ GeV, we can explain the $R_{K^{(*)}}$ anomaly since our Z' does not couple to electrons but to muons, resulting in the violation of lepton flavor universality. Large mass splitting between $N_\pm$ states are favored for large $C_9^{\mu,\mathrm{NP}}$. The constraints on $b \to s$ transition from $b \to s\gamma$ and $B_s - \overline{B_s}$ mixing can be evaded by taking relatively heavy (~ 3 TeV) $\widetilde{q}$ and sizable product of Yukawa couplings, $y_L^s y_L^b \sim 0.1$. We predict that the deviation from the SM predictions in $B \to K^* \nu\overline{\nu}$ process is hard to observe, which can be tested at Belle-II.

Our dark matter can provide the correct relic density via the annihilations of the Higgs resonance channel and $N_- N_- \to Z'Z'$ channel. The latter channel is naturally realized in our model because Z' is relatively light and has sizable gauge coupling with the dark fermions $N_\pm$. Our model can be tested by searching for Z' and new colored scalar at the LHC.

Appendix A. Loop functions

The effective $b - s - Z'$ vertex at zero momentum transfer is given by the loop function at zero momentum transfer,

$$\mathcal{V}_{sb}(x_-, x_+) = \frac{1}{4} + \sqrt{x_- x_+}\, j(x_-, x_+) - \frac{1}{2} k(x_-, x_+) + I(x_-) + I(x_+), \tag{A.1}$$

where $x_\mp = m_\mp^2/m_d^2$ and

$$j(x) = \frac{x \log x}{x-1},$$
$$k(x) = \frac{x^2 \log x}{x-1},$$
$$I(x) = \frac{-3x^2 + 4x - 1 + 2x^2 \log x}{8(x-1)^2}. \tag{A.2}$$

The above result was cross-checked with that of a similar model, that is, the neutralino contribution to charged lepton flavor violating $l_j^- \to l_i^- l_i^- l_i^+$ processes such as $\mu^- \to e^- e^- e^+$ via Z-penguin diagrams [82]. The difference between (A.1) and Eq. (25) of [82] can be explained by the differences in the two models: *i)* Z' has vector coupling to dark matter in our model while Z-boson couples to $V - A$ current of Higgsino in the MSSM, *ii)* Z' does not couple to quarks in our model while Z-boson does. The loop functions of j and k with more than one argument are defined recursively as

$$f(x_1, x_2, x_3, \cdots) \equiv \frac{f(x_1, x_3, \cdots) - f(x_2, x_3, \cdots)}{x_1 - x_2}, \tag{A.3}$$

where $f = j, k$. These multi-argument functions of j and k also appear as loop functions for the $\Delta B = 2$ box diagrams.

The loop function $J_1(x)$ for $b \to s\gamma$ is obtained to be

$$J_1(x) = \frac{1 - 6x + 3x^2 + 2x^3 - 6x^2 \log x}{12(1-x)^4}. \tag{A.4}$$

Acknowledgements

The author is grateful to Yuji Omura, Eibun Senaha, Jusak Tandean and Chaehyun Yu for useful discussions. This work is supported in part by National Research Foundation of Korea (NRF) Research Grant NRF-2015R1A2A1A05001869.

References

[1] S. Descotes-Genon, J. Matias, M. Ramon, J. Virto, Implications from clean observables for the binned analysis of $B- > K*\mu^+\mu^-$ at large recoil, J. High Energy Phys. 01 (2013) 048, arXiv:1207.2753.
[2] LHCb collaboration, R. Aaij, et al., Measurement of form-factor-independent observables in the decay $B^0 \to K^{*0}\mu^+\mu^-$, Phys. Rev. Lett. 111 (2013) 191801, arXiv:1308.1707.
[3] LHCb collaboration, R. Aaij, et al., Angular analysis of the $B^0 \to K^{*0}\mu^+\mu^-$ decay using 3 fb^{-1} of integrated luminosity, J. High Energy Phys. 02 (2016) 104, arXiv:1512.04442.
[4] Belle collaboration, A. Abdesselam, et al., Angular analysis of $B^0 \to K^*(892)^0\ell^+\ell^-$, in: Proceedings, LHCSki 2016 – A First Discussion of 13 TeV Results, Obergurgl, Austria, April 10–15, 2016, 2016, arXiv:1604.04042.
[5] Belle collaboration, S. Wehle, et al., Lepton-flavor-dependent angular analysis of $B \to K^*\ell^+\ell^-$, Phys. Rev. Lett. 118 (2017) 111801, arXiv:1612.05014.
[6] LHCb collaboration, R. Aaij, et al., Angular analysis and differential branching fraction of the decay $B_s^0 \to \phi\mu^+\mu^-$, J. High Energy Phys. 09 (2015) 179, arXiv:1506.08777.
[7] LHCb collaboration, R. Aaij, et al., Differential branching fractions and isospin asymmetries of $B \to K^{(*)}\mu^+\mu^-$ decays, J. High Energy Phys. 06 (2014) 133, arXiv:1403.8044.
[8] LHCb collaboration, R. Aaij, et al., Measurements of the S-wave fraction in $B^0 \to K^+\pi^-\mu^+\mu^-$ decays and the $B^0 \to K^*(892)^0\mu^+\mu^-$ differential branching fraction, J. High Energy Phys. 11 (2016) 047, arXiv:1606.04731.
[9] CMS collaboration, V. Khachatryan, et al., Angular analysis of the decay $B^0 \to K^{*0}\mu^+\mu^-$ from pp collisions at $\sqrt{s} = 8$ TeV, Phys. Lett. B 753 (2016) 424–448, arXiv:1507.08126.
[10] LHCb collaboration, R. Aaij, et al., Differential branching fraction and angular analysis of $\Lambda_b^0 \to \Lambda\mu^+\mu^-$ decays, J. High Energy Phys. 06 (2015) 115, arXiv:1503.07138.
[11] G. Hiller, F. Kruger, More model-independent analysis of $b \to s$ processes, Phys. Rev. D 69 (2004) 074020, arXiv:hep-ph/0310219.
[12] LHCb collaboration, R. Aaij, et al., Test of lepton universality using $B^+ \to K^+\ell^+\ell^-$ decays, Phys. Rev. Lett. 113 (2014) 151601, arXiv:1406.6482.
[13] LHCb collaboration, R. Aaij, et al., Test of lepton universality with $B^0 \to K^{*0}\ell^+\ell^-$ decays, arXiv:1705.05802.
[14] S. Descotes-Genon, J. Matias, J. Virto, Understanding the $B \to K^*\mu^+\mu^-$ anomaly, Phys. Rev. D 88 (2013) 074002, arXiv:1307.5683.
[15] W. Altmannshofer, C. Niehoff, P. Stangl, D.M. Straub, Status of the $B \to K^*\mu^+\mu^-$ anomaly after Moriond 2017, Eur. Phys. J. C 77 (2017) 377, arXiv:1703.09189.
[16] B. Capdevila, A. Crivellin, S. Descotes-Genon, J. Matias, J. Virto, Patterns of New Physics in $b \to s\ell^+\ell^-$ transitions in the light of recent data, arXiv:1704.05340.
[17] A.K. Alok, D. Kumar, J. Kumar, R. Sharma, Lepton flavor non-universality in the B-sector: a global analyses of various new physics models, arXiv:1704.07347.
[18] M. Ciuchini, A.M. Coutinho, M. Fedele, E. Franco, A. Paul, L. Silvestrini, et al., On flavourful easter eggs for new physics hunger and lepton flavour universality violation, arXiv:1704.05447.
[19] A.K. Alok, B. Bhattacharya, A. Datta, D. Kumar, J. Kumar, D. London, New physics in $b \to s\mu^+\mu^-$ after the measurement of R_{K^*}, arXiv:1704.07397.

[20] Q. Chang, X.-Q. Li, Y.-D. Yang, A comprehensive analysis of hadronic b → s transitions in a family non-universal Z-prime model, J. Phys. G 41 (2014) 105002, arXiv:1312.1302.

[21] A. Crivellin, G. D'Ambrosio, J. Heeck, Addressing the LHC flavor anomalies with horizontal gauge symmetries, Phys. Rev. D 91 (2015) 075006, arXiv:1503.03477.

[22] B. Allanach, F.S. Queiroz, A. Strumia, S. Sun, Z' models for the LHCb and $g-2$ muon anomalies, Phys. Rev. D 93 (2016) 055045, arXiv:1511.07447.

[23] S.M. Boucenna, A. Celis, J. Fuentes-Martin, A. Vicente, J. Virto, Non-abelian gauge extensions for B-decay anomalies, Phys. Lett. B 760 (2016) 214–219, arXiv:1604.03088.

[24] S.M. Boucenna, A. Celis, J. Fuentes-Martin, A. Vicente, J. Virto, Phenomenology of an $SU(2)\times SU(2)\times U(1)$ model with lepton-flavour non-universality, J. High Energy Phys. 12 (2016) 059, arXiv:1608.01349.

[25] J. Kawamura, S. Okawa, Y. Omura, Impact of the $b\to sll$ anomalies on dark matter physics, arXiv:1706.04344.

[26] I. Garcia Garcia, LHCb anomalies from a natural perspective, J. High Energy Phys. 03 (2017) 040, arXiv:1611.03507.

[27] P. Ko, T. Nomura, H. Okada, A flavor dependent gauge symmetry, Predictive radiative seesaw and LHCb anomalies, arXiv:1701.05788.

[28] P. Ko, T. Nomura, H. Okada, Explaining $B\to K^{(*)}\ell^+\ell^-$ anomaly by radiatively induced coupling in $U(1)_{\mu-\tau}$ gauge symmetry, Phys. Rev. D 95 (2017) 111701, arXiv:1702.02699.

[29] P. Ko, Y. Omura, Y. Shigekami, C. Yu, LHCb anomaly and B physics in flavored Z' models with flavored Higgs doublets, Phys. Rev. D 95 (2017) 115040, arXiv:1702.08666.

[30] S.F. King, Flavourful Z' models for $R_{K^{(*)}}$, arXiv:1706.06100.

[31] S. Di Chiara, A. Fowlie, S. Fraser, C. Marzo, L. Marzola, M. Raidal, et al., Minimal flavor-changing Z' models and muon $g-2$ after the R_{K^*} measurement, arXiv:1704.06200.

[32] R. Alonso, P. Cox, C. Han, T.T. Yanagida, Anomaly-free local horizontal symmetry and anomaly-full rare B-decays, arXiv:1704.08158.

[33] C. Bonilla, T. Modak, R. Srivastava, J.W.F. Valle, $U(1)_{B_3-3L_\mu}$ gauge symmetry as the simplest description of $b\to s$ anomalies, arXiv:1705.00915.

[34] J. Ellis, M. Fairbairn, P. Tunney, Anomaly-free models for flavour anomalies, arXiv:1705.03447.

[35] R. Alonso, P. Cox, C. Han, T.T. Yanagida, Flavoured $B-L$ local symmetry and anomalous rare B decays, arXiv:1705.03858.

[36] Y. Tang, Y.-L. Wu, Flavor non-universality gauge interactions and anomalies in B-meson decays, arXiv:1705.05643.

[37] A. Datta, J. Kumar, J. Liao, D. Marfatia, New light mediators for the R_K and R_{K^*} puzzles, arXiv:1705.08423.

[38] C.-W. Chiang, X.-G. He, J. Tandean, X.-B. Yuan, $R_{K^{(*)}}$ and related $b\to s\ell\bar{\ell}$ anomalies in minimal flavor violation framework with Z' boson, arXiv:1706.02696.

[39] D. Choudhury, A. Kundu, R. Mandal, R. Sinha, Minimal unified resolution to $R_{K^{(*)}}$ and $R(D^{(*)})$ anomalies with lepton mixing, arXiv:1706.08437.

[40] M. Bauer, M. Neubert, Minimal leptoquark explanation for the $R_{D^{(*)}}$, R_K, and $(g-2)_g$ anomalies, Phys. Rev. Lett. 116 (2016) 141802, arXiv:1511.01900.

[41] D. Das, C. Hati, G. Kumar, N. Mahajan, Towards a unified explanation of $R_{D^{(*)}}$, R_K and $(g-2)_\mu$ anomalies in a left-right model with leptoquarks, Phys. Rev. D 94 (2016) 055034, arXiv:1605.06313.

[42] D. Bečirević, S. Fajfer, N. Košnik, O. Sumensari, Leptoquark model to explain the B-physics anomalies, R_K and R_D, Phys. Rev. D 94 (2016) 115021, arXiv:1608.08501.

[43] S. Sahoo, R. Mohanta, A.K. Giri, Explaining the R_K and $R_{D^{(*)}}$ anomalies with vector leptoquarks, Phys. Rev. D 95 (2017) 035027, arXiv:1609.04367.

[44] G. Hiller, D. Loose, K. Schönwald, Leptoquark flavor patterns & B decay anomalies, J. High Energy Phys. 12 (2016) 027, arXiv:1609.08895.

[45] B. Bhattacharya, A. Datta, J.-P. Guévin, D. London, R. Watanabe, Simultaneous explanation of the R_K and $R_{D^{(*)}}$ puzzles: a model analysis, J. High Energy Phys. 01 (2017) 015, arXiv:1609.09078.

[46] D. Bečirević, O. Sumensari, A leptoquark model to accommodate $R_K^{\rm exp}<R_K^{\rm SM}$ and $R_{K^*}^{\rm exp}<R_{K^*}^{\rm SM}$, arXiv:1704.05835.

[47] Y. Cai, J. Gargalionis, M.A. Schmidt, R.R. Volkas, Reconsidering the One Leptoquark solution: flavor anomalies and neutrino mass, arXiv:1704.05849.

[48] D. Das, C. Hati, G. Kumar, N. Mahajan, Scrutinizing R-parity violating interactions in light of $R_{K^{(*)}}$ data, arXiv:1705.09188.

[49] G. Bélanger, C. Delaunay, S. Westhoff, A dark matter relic from muon anomalies, Phys. Rev. D 92 (2015) 055021, arXiv:1507.06660.

[50] B. Gripaios, M. Nardecchia, S.A. Renner, Linear flavour violation and anomalies in B physics, J. High Energy Phys. 06 (2016) 083, arXiv:1509.05020.

[51] Q.-Y. Hu, X.-Q. Li, Y.-D. Yang, $B^0\to K^{*0}\mu^+\mu^-$ decay in the aligned two-Higgs-doublet model, Eur. Phys. J. C 77 (2017) 190, arXiv:1612.08867.

[52] G. D'Amico, M. Nardecchia, P. Panci, F. Sannino, A. Strumia, R. Torre, et al., Flavour anomalies after the R_{K^*} measurement, arXiv:1704.05438.

[53] J.F. Kamenik, Y. Soreq, J. Zupan, Lepton flavor universality violation without new sources of quark flavor violation, arXiv:1704.06005.

[54] Z. Poh, S. Raby, Vector-like leptons: muon g-2 anomaly, lepton flavor violation, higgs decays, and lepton non-universality, arXiv:1705.07007.

[55] X.G. He, G.C. Joshi, H. Lew, R.R. Volkas, NEW Z-prime PHENOMENOLOGY, Phys. Rev. D 43 (1991) 22–24.

[56] X.-G. He, G.C. Joshi, H. Lew, R.R. Volkas, Simplest Z-prime model, Phys. Rev. D 44 (1991) 2118–2132.

[57] S. Baek, N.G. Deshpande, X.G. He, P. Ko, Muon anomalous g-2 and gauged L(muon) - L(tau) models, Phys. Rev. D 64 (2001) 055006, arXiv:hep-ph/0104141.

[58] S. Baek, P. Ko, Phenomenology of U(1) (L(mu)-L(tau)) charged dark matter at PAMELA and colliders, J. Cosmol. Astropart. Phys. 0910 (2009) 011, arXiv:0811.1646.

[59] S. Baek, H. Okada, K. Yagyu, Flavour dependent gauged radiative neutrino mass model, J. High Energy Phys. 04 (2015) 049, arXiv:1501.01530.

[60] S. Baek, Dark matter and muon $(g-2)$ in local $U(1)_{L_\mu-L_\tau}$-extended Ma Model, Phys. Lett. B 756 (2016) 1–5, arXiv:1510.02168.

[61] W. Altmannshofer, S. Gori, M. Pospelov, I. Yavin, Quark flavor transitions in $L_\mu-L_\tau$ models, Phys. Rev. D 89 (2014) 095033, arXiv:1403.1269.

[62] A. Crivellin, G. D'Ambrosio, J. Heeck, Explaining $h\to\mu^\pm\tau^\mp$, $B\to K^*\mu^+\mu^-$ and $B\to K\mu^+\mu^-/B\to Ke^+e^-$ in a two-Higgs-doublet model with gauged $L_\mu-L_\tau$, Phys. Rev. Lett. 114 (2015) 151801, arXiv:1501.00993.

[63] W. Altmannshofer, I. Yavin, Predictions for lepton flavor universality violation in rare B decays in models with gauged $L_\mu-L_\tau$, Phys. Rev. D 92 (2015) 075022, arXiv:1508.07009.

[64] P. Arnan, L. Hofer, F. Mescia, A. Crivellin, Loop effects of heavy new scalars and fermions in $b\to s\mu^+\mu^-$, J. High Energy Phys. 04 (2017) 043, arXiv:1608.07832.

[65] W. Altmannshofer, S. Gori, S. Profumo, F.S. Queiroz, Explaining dark matter and B decay anomalies with an $L_\mu-L_\tau$ model, J. High Energy Phys. 12 (2016) 106, arXiv:1609.04026.

[66] C.-H. Chen, T. Nomura, Penguin $b\to s\ell'^+\ell'^-$ and B-meson anomalies in a gauged $L_\mu-L_\tau$, arXiv:1707.03249.

[67] S. Baek, Z.-F. Kang, Naturally large radiative lepton flavor violating higgs decay mediated by lepton-flavored dark matter, J. High Energy Phys. 03 (2016) 106, arXiv:1510.00100.

[68] S. Baek, T. Nomura, H. Okada, An explanation of one-loop induced $h\to\mu\tau$ decay, Phys. Lett. B 759 (2016) 91–98, arXiv:1604.03738.

[69] S. Baek, P. Ko, P. Wu, Top-philic scalar dark matter with a vector-like fermionic top partner, J. High Energy Phys. 10 (2016) 117, arXiv:1606.00072.

[70] S. Baek, P. Ko, W.-I. Park, Search for the Higgs portal to a singlet fermionic dark matter at the LHC, J. High Energy Phys. 02 (2012) 047, arXiv:1112.1847.

[71] S. Baek, P. Ko, W.-I. Park, E. Senaha, Higgs portal vector dark matter: revisited, J. High Energy Phys. 05 (2013) 036, arXiv:1212.2131.

[72] Particle Data Group collaboration, C. Patrignani, et al., Rev. Part. Phys., Chin. Phys. C 40 (2016) 100001.

[73] LUX collaboration, D.S. Akerib, et al., Results from a search for dark matter in the complete LUX exposure, Phys. Rev. Lett. 118 (2017) 021303, arXiv:1608.07648.

[74] Y. Amhis, et al., Averages of b-hadron, c-hadron, and τ-lepton properties as of summer 2016, arXiv:1612.07233.

[75] M. Misiak, et al., Updated NNLO QCD predictions for the weak radiative B-meson decays, Phys. Rev. Lett. 114 (2015) 221801, arXiv:1503.01789.

[76] G. Buchalla, A.J. Buras, M.E. Lautenbacher, Weak decays beyond leading logarithms, Rev. Mod. Phys. 68 (1996) 1125–1144, arXiv:hep-ph/9512380.

[77] Particle Data Group collaboration, C. Patrignani, et al., Rev. Part. Phys., Chin. Phys. C 40 (2016) 100001.

[78] UTfit collaboration, M. Bona, et al., The unitarity triangle fit in the standard model and hadronic parameters from lattice QCD: a reappraisal after the measurements of Delta m(s) and BR(B –> tau nu(tau)), J. High Energy Phys. 10 (2006) 081, arXiv:hep-ph/0606167.

[79] J. Charles, et al., Current status of the standard model CKM fit and constraints on $\Delta F=2$ new physics, Phys. Rev. D 91 (2015) 073007, arXiv:1501.05013.

[80] T. Jubb, M. Kirk, A. Lenz, G. Tetlalmatzi-Xolocotzi, On the ultimate precision of meson mixing observables, Nucl. Phys. B 915 (2017) 431–453, arXiv:1603.07770.

[81] G. Bélanger, F. Boudjema, A. Pukhov, A. Semenov, micrOMEGAs4.1: two dark matter candidates, Comput. Phys. Commun. 192 (2015) 322–329, arXiv:1407.6129.

[82] J. Hisano, T. Moroi, K. Tobe, M. Yamaguchi, Lepton flavor violation via right-handed neutrino Yukawa couplings in supersymmetric standard model, Phys. Rev. D 53 (1996) 2442–2459, arXiv:hep-ph/9510309.